Glucose-evoked alterations in connexin43-mediated cell-to-cell communication in human collecting duct: a possible role in diabetic nephropathy

Claire E. Hills, Rosemary Bland, Dianne C. Wheelans, Jeanette Bennett, Pierre M. Ronco and Paul E. Squires

Am J Physiol Renal Physiol 291:1045-1051, 2006. First published May 9, 2006;
doi:10.1152/ajprenal.00344.2005

Am J Physiol Renal Physiol 291: F1045–F1051, 2006.
First published May 9, 2006; doi:10.1152/ajprenal.00344.2005.

Glucose-evoked alterations in connexin43-mediated cell-to-cell communication in human collecting duct: a possible role in diabetic nephropathy

Claire E. Hills,[1] Rosemary Bland,[1] Dianne C. Wheelans,[1] Jeanette Bennett,[1] Pierre M. Ronco,[2] and Paul E. Squires[1]

[1]*Molecular Physiology, Biomedical Research Institute, Department of Biological Sciences, University of Warwick, Coventry, United Kingdom; and* [2]*Unité Institut National de la Santé et de la Recherche Médicale, Universite de Paris, Hôpital Tenon (Assistance Publique-Hôpitaux de Paris), Paris, France*

Submitted 23 August 2005; accepted in final form 2 May 2006

Hills, Claire E., Rosemary Bland, Dianne C. Wheelans, Jeanette Bennett, Pierre M. Ronco, and Paul E. Squires. Glucose-evoked alterations in connexin43-mediated cell-to-cell communication in human collecting duct: a possible role in diabetic nephropathy. *Am J Physiol Renal Physiol* 291: F1045–F1051, 2006. First published May 9, 2006; doi:10.1152/ajprenal.00344.2005.—Aberrant sodium absorption has been linked to the development of hypertension in both renal disease and diabetes. Efficient absorption depends on coordination of cellular activity across the entire epithelium via cell-to-cell coupling. In the current study we have utilized a model human collecting duct cell line (HCD) to assess the role of connexin43 (Cx43)-mediated gap junctions in the transfer of intracellular Ca^{2+} transients within coupled cell clusters. HCD cells express Cx43 mRNA and protein, as well as that for the mechanosensitive transient receptor potential receptor (TRPV4). Mechanical stimulation of individual cells within a cluster evoked a transient rise in cytosolic Ca^{2+} concentration ($[Ca^{2+}]_i$) that propagated between cells via a heptanol-sensitive mechanism. The rise in $[Ca^{2+}]_i$ was dependent on both store release and Ca^{2+}-influx pathways. Lucifer yellow dye transfer and Cx43 knockdown experiments confirmed direct cell-to-cell communication. Application of the Ca^{2+} ionophore ionomycin, or an increase in glucose (5 to 25 mM), produced a time-dependent (48 h) increase in Cx43 protein expression. The transmission rate of touch-evoked Ca^{2+} transients between coupled cells was accelerated after exposure to high glucose, providing a functional correlate to increased Cx43 expression. These data suggest a pivotal role for Cx43-mediated gap junctions in the synchronization of activity between HCD cells in response to stimuli that mimic osmotic and physical changes. Cx43 expression and cell-to-cell communication increased in response to high glucose and may protect the collecting duct from renal damage associated with more established diabetic nephropathy.

gap junctions

THE TRANSIENT RECEPTOR POTENTIAL (TRP) superfamily of proteins are cation-selective ion channels that have diverse functions as cellular sensors (reviewed in Ref. 4). Mechanosensitive TRP proteins include TRP receptor (TRPV4) and are likely to be important in sensing both fluid flow and osmolarity in renal tubules (reviewed in Ref. 14) where they are known to evoke changes in cytosolic Ca^{2+} concentration ($[Ca^{2+}]_i$) (27). Gap junctions allow the transfer of ions and small molecules between coupled cells and enable individual cells to monitor the functional state of their immediate neighbors. Cell communication of this type permits an adaptation of function to match the immediate needs of coupled cells within a cluster (11). Gap junctions are composed of connexins, nine of which are known to be expressed in the kidney (9, 36). In the collecting duct of the nephron, connexin43 (Cx43) expression is the greatest (9). The presence of connexin-mediated gap junctions has been thought essential in kidney development and organogenesis; however, recent data from knockout mice lack evidence for dysplasia (30). A more likely and immediate role for gap junctions is in the coordination of activity between cells that, in isolation, would exhibit heterogeneous expression of key stimulus-response elements. Efficient and appropriate reabsorption of sodium within the cortical collecting duct (CCD) depends on an integrated response of the entire epithelium. Cell-to-cell coupling allows surrounding cells to lock into a particular frequency of cellular activity, ensuring a simultaneous response across the epithelial layer (5).

Mechanical stimulation increases $[Ca^{2+}]_i$ in a rat osteoblastic cell line (ROS). The resultant Ca^{2+} wave propagates into neighboring cells via heptanol-sensitive gap junctions (8). A similar response is seen in rat glomerular mesangial cells (37), rabbit CCD (20), and rat retinal epithelia (7). Dephosphorylation of Cx43 activates gap junctions (35) and in bladder smooth muscle Cx43 expression and cell coupling is increased in response to stretch (3). Clearly, Cx43 expression and the ability of cells to communicate are not static; however, the particular degree of compensation in response to various pathophysiological challenges remains confused. Injury or loss in a number of visceral epithelial cells of the renal glomeruli (podocytes) as a consequence of glomerulosclerosis or renal disease results in increased Cx43 expression in rats (38). This upregulation of Cx43 expression is also seen in inflammatory renal disease (13) and in the kidneys of hypertensive rats (10). However, compensatory renal growth in mice has been associated with a transient decrease gap-junction expression and cell-to-cell communication (18). Cell-to-cell communication within retinal microvessels is reduced in streptozotocin-induced diabetic rats (26), a situation also observed in vascular cells (16) and bovine aortic endothelial cells in response to elevated glucose (15, 17). These changes in connexin expression may have important repercussions for macrovascular dysfunction seen in diabetes, such as macroangiopathy, whereas the glucose-dependent

Address for reprint requests and other correspondence: P. E. Squires, Molecular Physiology, Biomedical Research Institute, Dept. of Biological Sciences, Univ. of Warwick, Coventry, CV4 7AL, UK (e-mail: psquires@bio.warwick.ac.uk).

The costs of publication of this article were defrayed in part by the payment of page charges. The article must therefore be hereby marked "*advertisement*" in accordance with 18 U.S.C. Section 1734 solely to indicate this fact.

downregulation of Cx43 protein expression and gap junctional-mediated intercellular communication between bovine retinal pericytes (19), endothelial cells (6), and rat retinal epithelial cells (7) indicates a role in microvascular complications, such as diabetic retinopathy.

In the current study we have utilized a human-derived collecting duct cell line (HCD) to assess the role of Cx43-mediated gap junctions in the transfer of touch-evoked Ca^{2+} waves between coupled cells to determine whether Cx43-mediated cell-to-cell coupling has a role in the development of secondary hypertension associated with elevated glucose as seen in diabetes mellitus.

MATERIALS AND METHODS

Cell culture. HCD cells were derived from normal human kidney cortex and immortalized with SV-40 virus. Clones were selected using the monoclonal antibody, Ab272, which specifically recognizes collecting duct principal cells. HCD cells (*passages 18–30*) were maintained in DMEM-Ham's F-12 medium (GIBCO, Invitrogen), supplemented with 2% FCS, 2 mmol/l glutamine, 15 mmol/l HEPES, 5 μg/ml transferrin, 5 ng/ml Na_2SeO_3, 5 μg/ml insulin, and 5×10^{-8} M dexamethasone. Cells were grown at 37°C in a humidified atmosphere of 5% CO_2 in air. For Ca^{2+} experiments, cells were seeded onto 3-aminopropyltriethoxysilane (APES; Sigma, Poole, UK)-treated coverslips and used within 1 day of plating. For glucose experiments, cells were treated with 5 or 25 mM glucose in the presence of unsupplemented DMEM-Ham's F-12 medium without FCS for time periods of 0, 24, and 48 h after FCS deprivation overnight. Basal (5 mM) glucose culture media was generated by mixing DMEM (0 mM glucose) with Ham's F-12 medium (10 mM glucose).

Analysis of mRNA expression. RNA was prepared from 80% confluent HCD cells by acid-guanidinium extraction (2) using a genelute mammalian total RNA miniprep kit (Sigma) following the manufacturer's instructions. Complementary DNA was synthesized by reverse transcription using a Promega Reverse Transcription System following an adapted method. Briefly, 1 μg of total RNA and 0.5 μg of random hexamers, in a final volume of 11 μl, were incubated at 70°C for 5 min and then allowed to cool slowly to 25°C. Primer extension was then performed at 37°C for 60 min after the addition of 1× (final concentration) reaction buffer, containing (in mmol/l) 50 Tris·HCl (pH 8.3), 50 KCl, 10 $MgCl_2$, 10 dithiothreitol, and 0.5 spermidine and 1 mmol/l (final concentration) of each dNTP, 40 U of rRNAsin ribonuclease inhibitor, and 15 U of avian myeloblastosis virus reverse transcriptase in a final volume of 20 μl. The RT mixture was heated to 95°C for 5 min and then 4°C for 5 min. An aliquot of 4 μl was used in subsequent PCR reactions.

PCR amplification of cDNAs. Amplification of specific cDNAs was carried out using the primers listed in Table 1. PCR reactions (20 μl) were set up containing 1.5 mmol/l $MgCl_2$, 0.2 mmol/l of each dNTP, 0.5 μM of each primer, and 1 U *Taq* DNA polymerase (Bioline). Amplification of samples was performed using an initial denaturation step of 95°C (5 min), followed by either 34 cycles (TRPV4) or 30 cycles (Cx43) consisting of 1 min of denaturing at 95°C, 1 min of annealing at the required temperature (Table 1), and a 1-min extension at 72°C. A final elongation step of 72°C for 7 min was included in all PCR amplifications.

Table 1. *PCR primers used to amplify TRPV4 and Cx43 mRNA*

mRNA	Primers (5′→3′)	Direction	Annealing Temperature, °C	Product Size, bp
TRPV4	CCCGTGAGAACACCAAGTTT	F	58	618
	TCACTCCAGGGCATTTCTTC	R		
Cx43	ATGAGCAGTCTGCCTTTCGT	F	58	597
	GGTCGCTCTTTCCCTTAACC	R		

TRPV4, transient receptor potential recepter; Cx43, connexin43; F, forward primer; R, reverse primer.

Analysis of protein expression. The preparation of cytosolic proteins and their subsequent separation by gel electrophoresis and electroblotting onto Immobilon-P membrane (Millipore, Watford, UK) were as described previously (1). Briefly, proteins (5 μg) were separated by SDS polyacrylamide gel electrophoresis (4.5% stacking gel, 7.5 or 10% resolving gel) at 200 V for 50 min in electrophoresis buffer containing 25 mmol/l Tris, 192 mmol/l glycine, and 0.1% (wt/vol) SDS. Proteins were transferred onto Immobilin-P membrane in transfer buffer [25 mmol/l Tris, 192 mmol/l glycine, 20% (vol/vol) methanol] for 1 h at 100 V at 4°C. After protein transfer, membranes were blocked in PBS plus 0.1% Tween 20 (PBS-T) containing 20% (wt/vol) nonfat milk powder (Marvel, Premier Brands, Stafford, UK) for 1 h at 25°C and then washed with PBS-T for 15 min. Filters were analyzed with specific polyclonal antibodies against human Cx43 (Santa Cruz Biotechnology) and TRPV4 (The Binding Site, Birmingham, UK) diluted in PBS-T (0.05%) at 1:200 and 1:1,000, respectively. After three 10-min washes in PBS-T, the membranes were incubated with the secondary antibody (horseradish peroxidase-conjugated) anti-rabbit (Cx43, diluted 1:2,000) and anti-sheep (TRPV4, diluted 1:30,000) in PBS-T (0.05%) for 60 min at 25°C, followed by three 10-min washes in PBS-T. Specific proteins were detected using ECL detection reagent chemiluminescence system (Amersham Biosciences) and were visualized after exposure of membranes to X-ray film for 1–10 min of Cx43 and TRPV4. Control experiments were included where primary antibody was omitted, and filters were exposed to secondary antibody and ECL detection.

Immunocytochemistry. Cells were allowed to grow to 80% confluence on APES-treated coverslips and then fixed in 4% paraformaldehyde. Nonspecific binding was prevented by blocking for 1 h at 25°C in PBS + 0.01% Triton X-100 containing 10% normal goat serum. After three 10-min washes with PBS, the nuclear stain 4′,6-diamidino-2-phenylindole dihydrochloride (1 mmol/l) was added to each coverslip for 3 min. After being washed with PBS (3 × 5 min), cells were incubated with the cytoskeletal stain tetramethylrhodamine isothiocynate-conjugated phalloidin (Sigma) diluted at 1:100 in PBS supplemented with 0.01% Triton X-100 for 1 h at 25°C. After being further washed (3 × 5 min), cells were incubated overnight at 4°C with the corresponding primary antibody (anti-Cx43, 1:100) diluted in PBS + 0.01% Triton X-100. After antibody incubation, cells were washed with PBS and then incubated in Alexa 488-conjugated goat anti-rabbit (Cx43) for 1 h at 25°C. Secondary antibodies (Molecular Probes) were diluted (1:400) in PBS + 0.01% Triton X-100. After 1 h, cells were washed 3 × 10 min and coverslips were mounted in Citifluor (glycerol-PBS solution: Agar Scientific) on glass slides.

Knockdown of Cx43 expression. Cells were allowed to grow to 40% confluence in six-well plates or APES-treated coverslips. Knockdown of Cx43 expression was achieved by two different small interfering RNA (siRNA) protocols.

First, there was transfection of cells with a pool of four Cx43 specific siRNA duplexes (Santa Cruz Biotechnology). Transfection of siRNAs was carried out using Lipofectamine (Invitrogen), following the manufacturer's instructions. Briefly, Lipofectamine and siRNAs were diluted into OptiMEM medium (Invitrogen). Diluted Lipofectamine lipids were mixed with diluted siRNAs, and the mixture was incubated for 30 min at room temperature for complex formation. Mixtures were further diluted in OptiMEM and added to each well, such that the final concentration of siRNAs was 80 nM. Cells were harvested and assayed 24 h after transfection. Negative controls included untransfected cells, lipid alone, two scrambled siRNAs, one of which was fluorscein conjugated (Santa Cruz Biotechnology).

Second, there was the siLentGene U6 Cassette RNA Interference System (Promega). Specific Cx43 and scrambled sequences were selected using the Promega design tool. U6 expression cassettes were

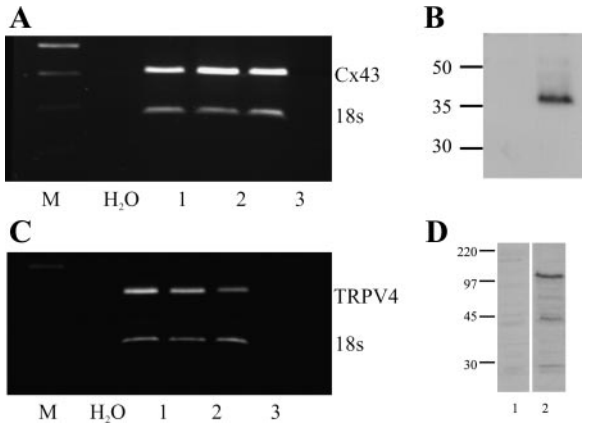

Fig. 1. Expression of transient receptor potential receptor (TRPV4) and connexin43 (Cx43) mRNA and protein in human collecting duct (HCD) cells. *A* and *C*: RT-PCR analyses using primers specific for human Cx43 and TRPV4. PCR products of 597 and 618 bp were observed in 3 RNA preparations (1, 2, and 3) corresponding to mRNA expression for Cx43 and TRPV4 in HCD cells. Negative controls included both water and samples in which avian myeloblastosis virus enzyme had been omitted from reverse transcription reaction. Western blot analyses of HCD cell lysates (*B* and *D*, 5 μg protein/lane) using an antibody against human Cx43 (*B*, *lane 2*) and TRPV4 (*D*, *lane 2*) confirmed the presence of the proteins. A protein band of ~43 (Cx43) and 120 kDa (TRPV4) was detected. Controls included protein from cells transfected with Cx43 small interfering RNA (siRNA) (*B*, *lane 1*) and TRPV4 antibody preabsorbed with a 100-fold excess of immunizing peptide (*D*, *lane 1*). M, marker.

constructed following the manufacturer's instructions. Transfection of the U6 DNA expression cassettes was performed using siLentGene transfection reagent (Promega), such that the final concentration of cassettes was 160 ng/ml. To localize transfected cells, cells were cotransfected with red fluorescent protein (RFP; pDsRed2-C1). Cells were harvested and assayed 72 h after transfection. Negative controls included untransfected cells, lipid alone, RFP alone, and a scrambled siRNA.

In each case Cx43 knockdown was confirmed by Western blot analysis as described above.

Single-cell microfluorimetry. HCD cells seeded and grown overnight on APES-coated coverslips were loaded for 30 min at 37°C with 2.5 μM of the Ca^{2+} fluorophore fura-2 AM (Sigma). Coverslips were washed and placed in a steel chamber, the volume of which was ~500 μl. A single 22-mm coverslip formed the base of the chamber, which was mounted into a heating platform on the stage of an Axiovert 200 Research Inverted microscope (Carl Zeiss, Welwyn Garden City, UK). All experiments were carried out at 37°C using unsupplemented DMEM-Ham's F-12 medium as the standard extracellular medium. Cells were illuminated alternatively at 340 and 380 nm using a Metaflour imaging workbench (Universal Imaging, Marlow, Bucks, UK). Emitted light was filtered by using a 510-nm long-pass barrier filter and detected using a Cool Snap HQ CCD camera (Roper Scientific). Changes in the emission intensity of fura-2 expressed as a ratio of dual excitation were used as an indicator of changes in $[Ca^{2+}]_i$ with the use of established procedures. Data were collected at 3-s intervals for multiple regions of interest in any one field of view. All records have been corrected for background fluorescence (determined from cell-free coverslip).

Mechanical stimulation of HCD cells. Individual cells within a cluster (6–12 cells/cluster) of fura-2-loaded cells were stimulated via touch using a femtotip electrode delivery system (Eppendorf, Hamburg, Germany). Maintained fura-2 fluorescence confirmed the integrity of the cell membrane.

Transmission velocity experiments. HCD cells were seeded and grown to 50% confluence on APES-coated coverslips in the previously described standard culture medium. After an overnight period of serum starvation, the medium was then removed and changed to a test medium containing 5 or 25 mmol/l glucose. After a 24- or 48-h exposure to each test medium, individual cells within a cluster (6–12 cells/cluster) of fura-2-loaded cells were stimulated via touch using a femtotip electrode delivery system. The rate of transmission of a touch-evoked Ca^{2+} signal between individual HCD cells was assessed. Maintained fura-2 fluorescence confirmed the integrity of the cell membrane.

Dye transfer experiments. An individual cell within a cell cluster was microinjected with the membrane impermeant fluorescent tracer Lucifer yellow CH, dilithium salt (Sigma). Lucifer yellow was dissolved in 250 μl of fresh LiC (150 mmol/l)-HEPES (10 mmol/l; pH 7.2). Cells were injected using femtotips (internal diameter, 0.5 ± 0.2 μm) and the Injectman/Femtojet 5247 delivery system (Eppendorf, Hamburg, Germany). The duration for injections was set at 3 s at an injection pressure of 2 psi and a compensation pressure of 0.7 psi. Dye transfer was recorded over a subsequent 10-min period using Metamorph acquisition software (Universal Imaging) and a Cool Snap HQ CCD camera (Roper Scientific).

Data analysis. Autoradiographs were quantified by densitometry (TotalLab 2003). Statistical analysis of data was performed by using a one-way ANOVA test with a Tukey's multiple comparison posttest. Data are expressed as arithmetic means ± SE, *n* denotes the number of experiments, and $P < 0.05$ signifies statistical significance.

RESULTS

Expression and localization of Cx43 and TRPV4 in HCD cells. Studies confirmed the presence of Cx43 and TRPV4 mRNA and protein in HCD cells. RT-PCR analysis of several RNA preparations from HCD cells revealed PCR products representative of Cx43 and TRPV4 mRNA (Fig. 1, *A* and *C*, respectively). To confirm that both sets of mRNA were appropriately translated, protein expression was determined by Western blot analysis (Fig. 1, *B* and *D*). Western blot analyses revealed bands at ~43 and 120 kDa, representative of those expected for Cx43 and TRPV4, respectively. The distribution of Cx43 in HCD cells was examined by immunocytochemistry (Fig. 2). Cx43 protein expression was localized to the cell membrane with intense perinuclear staining.

Touch-evoked changes in cytosolic Ca^{2+} in HCD cells. Physical stimulation of a single HCD cell evoked an increase in cytosolic Ca^{2+} (Fig. 3, *A* and *B*). The response was rapid in onset but transient, with $[Ca^{2+}]_i$ returning to basal levels even in the presence of continued stimulus. The transmission of a $[Ca^{2+}]_i$ signal away from the point of stimulation (Fig. 3*A*; 0–6 s) illustrates cooperativity between HCD cells and is indicative of a high degree of cell-to-cell communication (data are representative of 5 separate experiments). Cell-to-cell com-

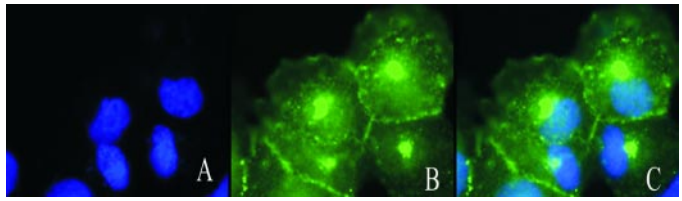

Fig. 2. Immunocytochemical staining of Cx43 in HCD cells. HCD cells were subjected to immunofluorescence staining with a polyclonal antibody against human Cx43. *A* and *B*: nuclear 4′,6-diamidino-2-phenylindole dihydrochloride (DAPI) and Cx43 staining, respectively. *C*: overlay of Cx43 immunolocalization (green) and nuclear staining (DAPI; blue). Note the intense Cx43 staining at cell periphery.

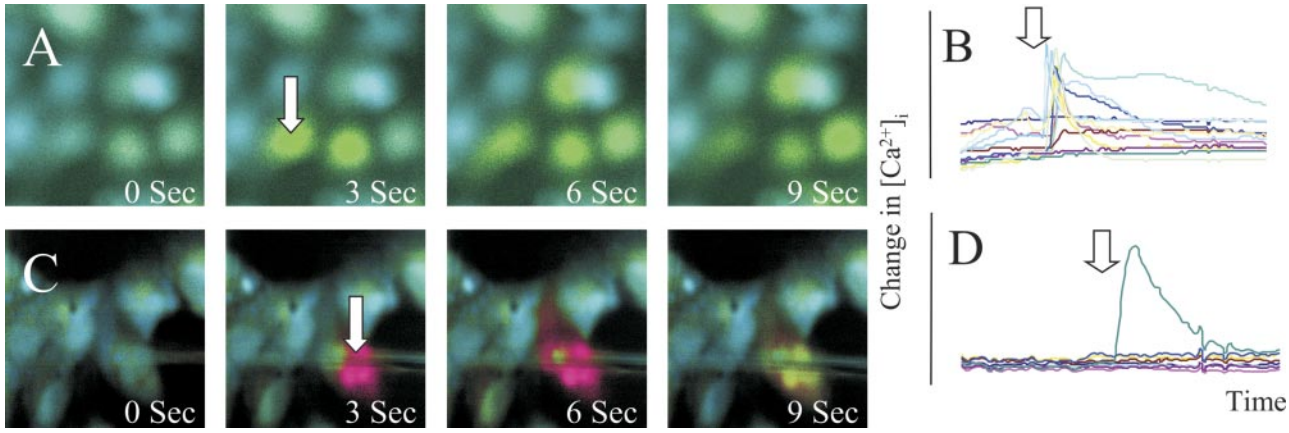

Fig. 3. Changes in cytosolic Ca^{2+} concentration ($[Ca^{2+}]_i$) in HCD cells evoked by mechanical stimulation. *A*: rapid spread of a touch-evoked Ca^{2+} transient within 16 cell clusters of HCD cells. A single cell is mechanically stimulated at 0 s. The evoked Ca^{2+} signal propagates away from point of stimulation into adjacent cells (2, 4, and 6 s). Elevation in $[Ca^{2+}]_i$ in each cell is shown in *B*. *C*: data from a similar experiment in a cluster of 8 HCD cells after application of gap-junctional uncoupler heptanol. Note that over a similar time (in s) course (0–6 s), touch-evoked changes in $[Ca^{2+}]_i$ no longer propagate into adjacent cells. These data are confirmed in *D*, which shows lack of Ca^{2+} response in all cells except that cell directly stimulated by mechanical stress. Data are represented as estimated change in cytosolic Ca^{2+} (change in $[Ca^{2+}]_i$) recorded as a ratio of 340- to 380-nm excitation for fura-2.

munication is not dependent on ATP-mediated paracrine mechanisms as an application of suramin [50 μM; a concentration known to block P_2 purinergic receptors (12)] failed to negate touch-evoked changes in intracellular Ca^{2+} (in 3 separate experiments; data not shown).

Gap junctions permit the free passage of both ions and small molecules between cells. To assess whether HCD cells express functional gap junctions, we examined the effect of the gap-junction uncoupler heptanol (1 mmol/l) on the propagation of touch-evoked Ca^{2+} signals. In the presence of heptanol, physical stimulation of an individual HCD cell within a cell cluster evoked a transient rise in cytosolic Ca^{2+} that failed to propagate into adjacent cells (Fig. 3, *C* and *D*). Results are representative of five separate experiments.

Touch-evoked changes in $[Ca^{2+}]_i$ were still observed under Ca^{2+}-free conditions (+EGTA, 1 mmol/l), although the basal-to-peak amplitude of the response was only 41% of that obtained in the presence of extracellular Ca^{2+} [100 ± 16% ($-Ca^{2+}$) compared with 244 ± 21% ($+Ca^{2+}$), $P < 0.05$, $n = 4$ separate experiments for each treatment; data not shown].

Dye transfer between cells. Lucifer yellow is a low molecular weight, membrane-impermeant, fluorescent compound. Propagation of the dye from an injected cell occurs via direct transfer through gap junctions. To further determine the role of gap junctions in cell-to-cell communication within our model, Lucifer yellow was injected into an individual HCD cell, and the dye spread within the cell cluster was monitored. As seen in Fig. 4*A*, within 3 min Lucifer yellow had permeated away from the site of injection into coupled cells. Application of the gap-junctional uncoupler heptanol (1 mmol/l; Fig. 4*D*) prevented any dye spread between neighboring cells. Data are representative of three separate experiments.

Knockdown of Cx43 expression prevents cell-to-cell communication. Transiently transfecting cells with siRNA for Cx43 significantly reduced Cx43 protein expression in HCD cells to ~50% of control (Fig. 5, *A* and *B*; representative of 4 separate experiments). Mechanical stimulation of an individual cell within a cluster of anti-Cx43 transfected HCD cells evoked a transient increase in cytosolic Ca^{2+} that failed to propagate into neighboring cells (Fig. 5*C*; representative of 8 separate experiments). A similar experiment using scrambled siRNA (Fig. 5*D*; representative of 3 separate experiments) failed to negate cell-to-cell communication of Ca^{2+}-signals between coupled HCD cells. Cotransfection with RFP and anti-Cx43

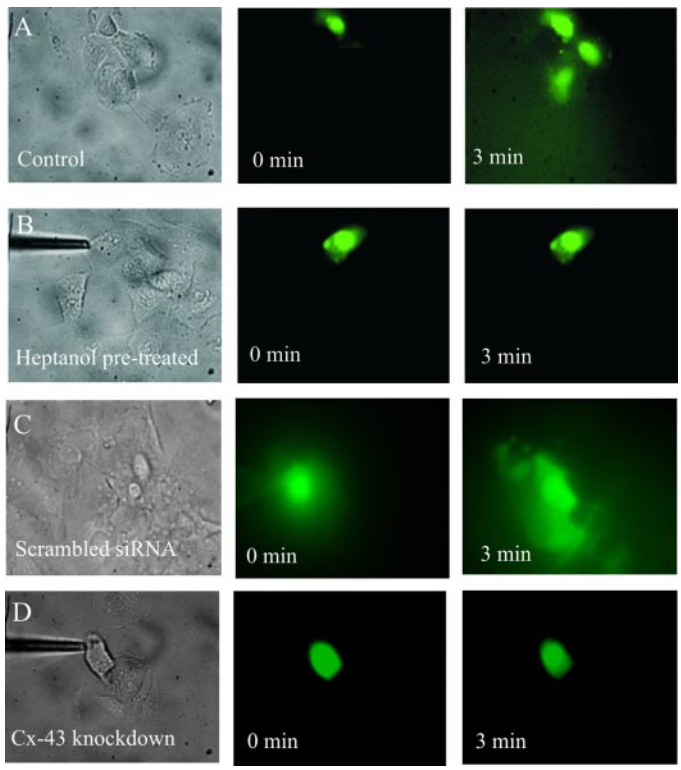

Fig. 4. Lucifer yellow dye transfer between HCD cells. Transfer of Lucifer yellow suggests direct cell-to-cell communication between coupled HCD cells. Monochrome plates illustrate phase images of HCD cell clusters. Fluorescence (fluorescein) image of same cell clusters after single-cell injection with Lucifer yellow is shown at 0 min. Same field of view is recorded 3 min after injection of dye in control cells (*A*), in the presence of heptanol (1 mM/l; *B*), in HCD cells transfected with scrambled siRNA (*C*), or in Cx43 knockdown HCD cells (*D*). Dye that spread into neighboring cells is only seen in control or scrambled siRNA cell clusters.

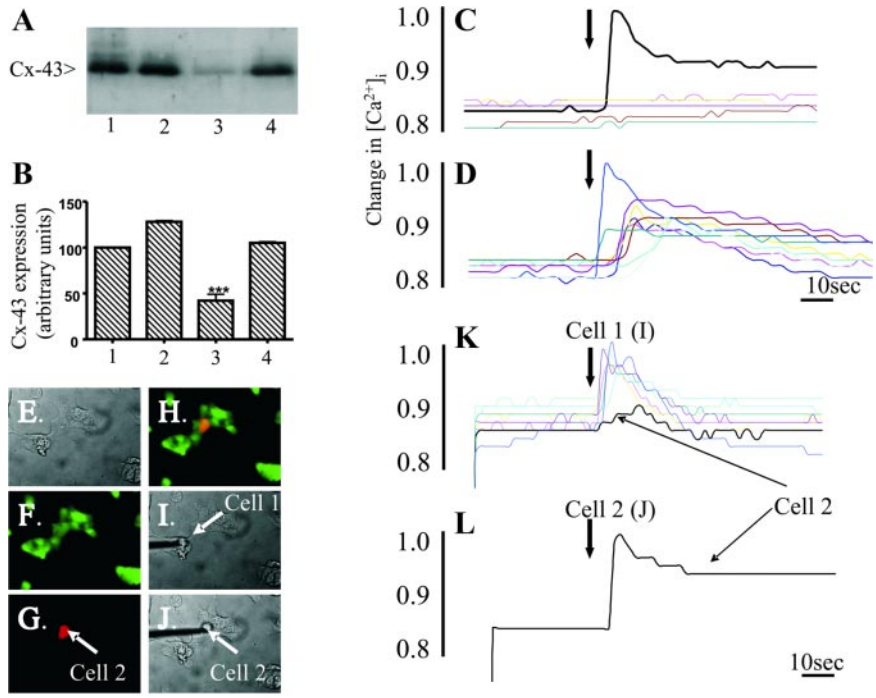

Fig. 5. Knockdown of Cx43 expression prevents intercellular communication of touch-evoked changes in $[Ca^{2+}]_i$. *A*: Western blot analyses of HCD cell lysates (5 μg protein/lane) using an antibody against human Cx43 (43 kDa) confirmed siRNA knockdown of Cx43 expression in *lane 3* compared with that in control cells (*lane 1*, untransfected cells; *lane 2*, cells transfected with lipid alone; *lane 4*, cells transfected with scrambled siRNA). Knockdown reduced Cx43 expression to ~50% of control (*B*). ***$P < 0.001$. Mechanical stimulation of an individual cell within a cluster of anti-Cx43 transfected HCD cells evoked a transient increase in cytosolic Ca^{2+} that failed to propagate into neighboring cells (*C*). Similar experiment using scrambled siRNA (*D*) fails to negate cell-to-cell communication of Ca^{2+} signals between coupled HCD cells. *E–L*: various images of a HCD cell cluster after cotransfection with anti-Cx43 siRNA and red fluorescent protein (RFP) using the siLentGene U6 Cassette RNA Interference System (Promega). Cell cluster was visualized either as a phase image (*E*, *I*, and *J*) loaded with fura-2 (*F*), optimized for RFP (*G*), and as an overlay of fura-2 fluorescence and RFP (*H*). An RFP-transfected cell (*cell 2* in *G*) is clearly identified in the fura-2-loaded cluster (*H*). Mechanical stimulation of a nontransfected cell (*cell 1* in *I*) evoked an increase in $[Ca^{2+}]_i$ that propagated between other nontransfected coupled cells (*K*). Touch-evoked signal failed to significantly elevate $[Ca^{2+}]_i$ in the RFP-tagged *cell 2*. To confirm cell viability after transfection, microelectrode was repositioned to stimulate transfected *cell 2* (*J*). Mechanical stimulation of *cell 2* elicited a rapid increase in $[Ca^{2+}]_i$ (*L*). These data suggest that knockdown of Cx43 expression reduces cell-to-cell communication in HCD cells. *C, D, K, L*: arrows denote point of mechanical stimulation.

identified single transfected cells within a cluster of HCD cells (Fig. 5, *G* and *H*; representative of 4 separate experiments). Mechanical stimulation of a nontransfected cell (*cell 1*) evoked an increase in $[Ca^{2+}]_i$ that propagated between other nontransfected coupled cells. The touch-evoked signal failed to significantly elevate $[Ca^{2+}]_i$ in the transfected cell (RFP-tagged *cell 2*; Fig. 5, *I* and *K*). However, mechanical stimulation of *cell 2* elicited a rapid increase in $[Ca^{2+}]_i$ (Fig. 5, *J* and *L*), indicating that Cx43 knockdown did not interfere with the ability of the cell to respond to touch. Transfection with lipid, RFP alone, or scrambled siRNA sequences did not alter responses to touch. These data suggest that knockdown of Cx43 expression reduces cell-to-cell communication in HCD cells.

Upregulation of Cx43 expression in high glucose and Ca^{2+}. To examine the effect of elevated glucose on Cx43 expression, HCD cells were incubated in high glucose (25 mM) for 24 and 48 h. Cells grown under these conditions exhibited increased Cx43 expression to 234 ± 12.7% of control (5 mM) at 48 h ($n = 3$, $P < 0.01$, see Fig. 6, *A* and *B*). In a similar series of experiments, to control for osmotic stress, mannitol (25 mM) increased Cx43 expression at 48 h by only 29% of the glucose-evoked change seen under identical experimental conditions (data not shown).

Cx43 expression has also been linked to increased $[Ca^{2+}]_i$ (33). Treatment of our HCD cells with the Ca^{2+} ionophore ionomycin (1 μM) significantly increased Cx43 expression at 4 h (211.5 ± 19.9%), 6 h (282.7 ± 18.5%), 8 h (403.7 ± 25.7%), 12 h (266 ± 8.7%), and 24 h (188.5 ± 1.82%; $P < 0.01$).

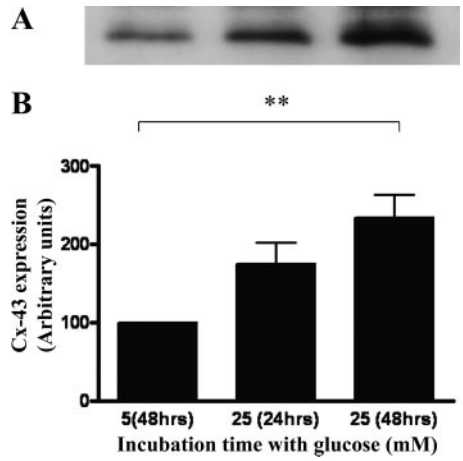

Fig. 6. Upregulation of Cx43 and protein expression in response to high glucose. HCD cells were incubated in 5 and 25 mM glucose for 24 and 48 h. *A*: representative Western blot analysis using an anti-Cx43 antibody. *B*: analysis of changes in Cx43 protein expression. Results represent means ± SE; number of experiments (n) = 4; **$P < 0.01$.

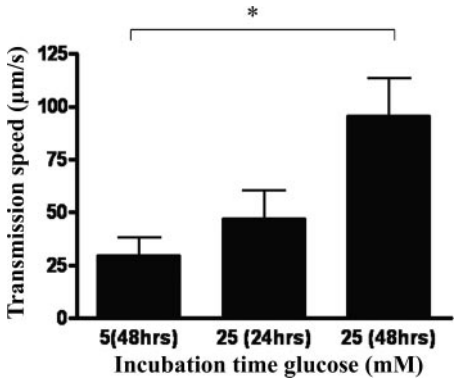

Fig. 7. Acceleration of touch-evoked Ca^{2+} signals between HCD cells by high glucose. HCD cells were incubated in 5 or 25 mM glucose for 24 and 48 h. Cells were then mechanically stimulated and the speed of transmission of the resultant Ca^{2+}-transient assessed (in μm/s). Data represent means ± SE, where *n* denotes the number of experiments, and $*P < 0.05$.

Acceleration of Ca^{2+} signals between HCD cells exposed to high glucose. The speed of propagating touch-evoked Ca^{2+} signals between adjacent cells in HCD clusters was significantly elevated after 48-h exposure to 25 mM glucose, compared with that of cells cultured in low (5 mM) glucose (321 ± 18.8%, $n = 3$; $P < 0.05$; see Fig. 7). These data suggest that increases in Cx43 expression in response to high glucose after 48 h facilitate improved signal transmission throughout the cluster.

DISCUSSION

The present study confirms that HCD cells express TRPV4 mechanoreceptors, and physical stimulation of HCD cells evoked a transient change in $[Ca^{2+}]_i$. These data are consistent with previous data linking membrane stretch in renal cells to an elevation in $[Ca^{2+}]_i$ as part of the regulatory cell volume decrease (23, 31, 32, 34). Mechanosensitive channels have a role in sodium reabsorption and regulate cell volume via Ca^{2+}-dependent mechanisms (26). Exposure of renal epithelial cells to changes in osmolality necessitates the initiation of cell volume regulatory processes, the activation of which serves to restore cell volume, preserving both integrity and functionality. The inability to resolve these changes may have serious repercussions for sodium transport and the development of secondary hypertension associated with renal diseases, such as diabetic nephropathy. The transfer of information regarding the osmotic state of the duct depends largely on cell-to-cell coupling. Consequently, changes in intercellular communication may play a key role in transducing changes in osmolarity to appropriate changes in absorption. Here, we examined the effect of touch on the generation of intracellular Ca^{2+} signals in a HCD cell line and investigated the role of Cx43-mediated gap junctions in propagating these signals under control and high glucose conditions.

In the current study, the rapid spread of touch-evoked Ca^{2+} transients (~30 μm/s) between neighboring cells and the movement of Lucifer yellow demonstrate a high degree of cell-to-cell communication, a supposition supported by the observation that HCD cells express the gap-junction subunit Cx43. Gap junctions are a class of membrane channels, which permit the passage of small ions and molecules from one cell to another. Cx43 immunoreactivity was localized to both the perinuclear and membrane region of HCD cells. Uncoupling of gap junctions, with the use of heptanol, attenuated the transfer of Ca^{2+} signals and dye spread between cells. Knockdown of Cx43 expression using siRNA technologies dramatically reduced the transfer of touch-evoked Ca^{2+} signals between adjacent HCD cells within cell clusters. This further supports the concept that there is a high degree of organization between cells of the collecting duct, which is, in part, mediated via the direct transfer of information.

Elevated glucose has been shown to decrease gap junctional conductance and disrupt cellular homeostasis in a variety of cell systems (24, 28). In streptozotocin-induced diabetic rats, dye spread in retinal microvessels was reduced in the absence of exogenous insulin (26). Similarly, glucose-dependent downregulation of Cx43 expression and gap-junctional intercellular communication (GJIC) has been reported in bovine retinal pericytes (19), endothelial (6), and epithelial cells (7, 21). Inoguchi et al. (15) and Kuroki et al. (17) demonstrated that 24-h exposure to high glucose evoked a protein kinase C-dependent decrease in GJIC in bovine aortic endothelial cells, a finding later supported by studies in streptozotocin-induced diabetic rats (16). However, the inhibitory effects of hyperglycemia on connexin-mediated cell-to-cell communication in various microvascular and macrovascular models are not so apparent in other tissues. In a rat osteosarcoma cell line, a 72-h exposure to 25 mM glucose had no effect on touch-evoked spread of Ca^{2+} transients (8), whereas it has been long established that high glucose increased the expression of gap junctions in pancreatic β-cells (22). In the current study, sub-48-h exposure of HCD cells to high (25 mM) glucose generated a marked increase in Cx43 protein expression and cell-to-cell transmission velocity for touch-evoked Ca^{2+} transients. Upregulation of Cx43 expression by glucose was only partially attributable to the osmotic effect of the sugar, because similar concentrations of mannitol produced only a 29% increase in Cx43 expression.

Cx43 expression has previously been linked to increased $[Ca^{2+}]_i$ (33). In the present study, Cx43 expression increased in response to elevated cytosolic Ca^{2+} after ionomycin treatment, and although this latter finding is opposite to that previously reported in osteoblast-like cells in culture, which showed reduced dye spread in the presence of the ionophore A-23187 (29), both studies suggest that the functional expression of gap junctions is Ca^{2+} dependent.

Increases in Cx43 functional expression coupling between cells may act to maintain epithelial integrity and prevent immediate and overt renal damage in the short term. Loss of this protection over time may contribute to the development of renal disease and diabetic nephropathy.

ACKNOWLEDGMENTS

C. E. Hills is a Biotechnology and Biological Sciences Research Council doctoral student. Equipment for single-cell work was supplied by Diabetes UK (RD01:0002216, to P. E. Squires). We thank Prof. A. R. Bradwell (The Binding Site, UK) for generating TRPV4 antibody and MRC Infrastructure Award (G4500017) "Bioinformatics and Structural Biology in The Life Sciences" for the TRPV4 peptide design.

GRANT

This work was supported by the Diabetes, Endocrine, and Immersion Research Trust (to R. Bland and P. E. Squires).

REFERENCES

1. **Bland R, Walker EA, Hughes SV, Stewart PM, and Hewison M.** Constitutive expression of 25-hydroxyvitamin D_3-1α-hydroxylase in a transformed human proximal tubule cell line: evidence for direct regulation of vitamin D metabolism by calcium. *Endocrinology* 140: 2027–2034, 1999.
2. **Chomczynski P and Sacchi N.** Single-step method of RNA isolation by acid guanidinium thiocyanate-phenol-chloroform extraction. *Anal Biochem* 162: 156–159, 1987.
3. **Christ GJ, Day NS, Day M, Zhao W, Persson K, Pandita RK, and Andersson KE.** Increased connexin43-mediated intercellular communication in a rat model of bladder overactivity in vivo. *Am J Physiol Regul Integr Comp Physiol* 284: R1241–R1248, 2003.
4. **Clapham DE.** TRP channels as cellular sensors. *Nature* 426: 517–524, 2003.
5. **De Blasio BF, Iversen JG, and Rottingen JA.** Intercellular calcium signalling in cultured renal epithelia: a theoretical study of synchronization mode and pacemaker activity. *Eur Biophys J* 33: 657–670, 2004.
6. **Fernandes R, Girao H, and Pereita P.** High glucose down-regulates intercellular communication in retinal endothelial cells by enhancing degradation of connexin 43 by a proteasome-dependent mechanism. *J Biol Chem* 279: 27219–27224, 2004.
7. **Gomes P, Malfait M, Himpens B, and Vereecke J.** Intercellular Ca^{2+}-transient propagation in normal and high glucose solutions in rat retinal epithelial (RPE-J) cells during mechanical stimulation. *Cell Calcium* 32: 185–192, 2003.
8. **Gomez P, Vereecke J, and Himpens B.** Intra- and intercellular Ca^{2+}-transient propagation in normal and high glucose solutions in ROS cells during mechanical stimulation. *Cell Calcium* 29: 137–148, 2000.
9. **Guo R, Liu L, and Barajas L.** RT-PCR study of the distribution of connexin 43 mRNA in the glomerulus and renal tubular segments. *Am J Physiol Regul Integr Comp Physiol* 275: R439–R447, 1998.
10. **Haefliger JA, Demotz S, Braissant O, Suter E, Waeber B, Nicod P, and Meda P.** Connexin 40 and 43 are differentially regulated within the kidneys of rats with renovascular hypertension. *Kidney Int* 60: 190–201, 2001.
11. **Haefliger JA, Nicod P, and Meda P.** Contribution of connexins to the function of the vascular wall. *Cardiovasc Res* 62: 345–356, 2004.
12. **Hauge-Evans AC, Squires PE, Belin VD, Roderigo-Milne RD, Ramracheya Persaud SJ, and Jones PM.** Role of adenine nucleotides in insulin secretion from MIN6 pseudoislets. *Mol Cell Endocrinology* 191: 167–176, 2002.
13. **Hilliis GS, Duthie LA, Brown PAJ, Simpson JG, Macleod AM, and Haites NE.** Upregulation and co-localization of connexin 43 and cellular adhesion molecules in inflammatory renal disease. *J Pathol* 182: 373–379, 1997.
14. **Huang CL.** The transient receptor potential superfamily of ion channels. *J Am Soc Nephrol* 15: 1690–1699, 2004.
15. **Inoguchi T, Ueda F, Umeda F, Yamashita T, and Nawata H.** Inhibition of intercellular communication via gap junction in cultured aortic endothelial cells by elevated glucose and phorbol ester. *Biochem Biophys Res Commun* 208: 492–497, 1995.
16. **Inoguchi T, Yan HY, Imamura M, Kakimoto M, Kuroki T, Maruyama T, and Nawata H.** Altered gap junction activity in cardiovascular tissues of diabetes. *Med Electron Microsc* 34: 86–91, 2001.
17. **Kuroki T, Inoguchi T, Umdea F, Ueda F, and Nawata H.** High glucose induces alteration of gap junction permeability and phosphorylation of connexin-43 in cultured aortic smooth muscle cells. *Diabetes* 47: 931–936, 1998.
18. **Li S, Nomata K, Hayashi T, Noguchi M, Kanda S, and Kanetake H.** Transient decrease in gap junction expression during compensatory renal growth in mice. *Urology* 60: 726–730, 2002.
19. **Li AF, Sato T, Haimovici R, Okamoto T, and Roy S.** High glucose alters connexin 43 expression and gap junction intercellular communication activity in retinal pericytes. *Invest Opthalmol Vis Sci* 44: 5376–5382, 2003.
20. **Liu W, Xu S, Woda C, Kim P, Weinbaum S, and Satin LM.** Effect of flow and stretch on the $[Ca^{2+}]_i$ response of principal and intercalated cells in cortical collecting duct. *Am J Physiol Renal Physiol* 285: F998–F1012, 2003.
21. **Malfait M, Gomez P, van Veen TAB, Parys JB, De Smedt H, Vereecke J, and Himpens B.** Effects of hyperglycaemia and protein kinase C on connexin 43 expression in cultured rat retinal pigment epithelial cells. *J Membr Biol* 181: 31–40, 2001.
22. **Meda P, Denef JF, Perrelet A, and Orci L.** Nonrandom distribution of gap junctions between pancreatic β-cells. *Am J Physiol Cell Physiol* 238: C114–C119, 1980.
23. **Montrose-Rafizdeh C and Guggino WB.** Role of intracellular calcium in volume regulation by rabbit medullary thick ascending limb cells. *Am J Physiol Renal Fluid Electrolyte Physiol* 260: F402–F409, 1991.
24. **Ngezahayo A and Kolb HA.** Gap junctional permeability is affected by cell volume changes and modulates volume regulation. *FEBS Lett* 276: 6–8, 1990.
25. **Nilius B, Vriens J, Prenen J, Droogmans G, and Voets T.** TRPV4 calcium entry channel: a paradigm for gating diversity. *Am J Physiol Cell Physiol* 286: C195–C205, 2004.
26. **Oku H, Kodama T, Sakagami K, and Puro DG.** Diabetes-induced disruption of gap-junction pathways within the retinal microvasculature. *Invest Ophthalmol Vis Sci* 42: 1915–1920, 2001.
27. **Praetorius HA and Spring KR.** The renal cell primary cilium functions as a flow sensor. *Curr Opin Nephrol Hypertens* 12: 129–137, 2003.
28. **Sato T, Haimovici R, Kao R, Li AF, and Roy S.** Downregulation of connexin 43 expression by high glucose reduces gap junction activity in microvascular endothelial cells. *Diabetes* 51: 1565–1571, 2002.
29. **Schirrmacher K, Nonhoff D, Wiemann M, Peterson-Grine E, Brink PR, and Bingmann D.** Effects of calcium on gap-junctions between osteoblast-like cells in culture. *Calcif Tissue Int* 59: 259–264, 1996.
30. **Silverstein DM, Urban M, Gao Y, Mattoo TK, Spray DC, and Rozental R.** Renal morphology in connexin 43 knockout mice. *Pediatr Nephrol* 16: 467–471, 2001.
31. **Tinel H, Wehner F, and Sauer H.** Intracellular Ca^{2+} release and Ca^{2+} influx during regulatory volume decrease in IMCD cells. *Am J Physiol Renal Fluid Electrolyte Physiol* 267: F130–F138, 1994.
32. **Tinel H, Kinne-Saffran E, and Kinne RKH.** Calcium signaling during RVD of kidney cells. *Cell Physiol Biochem* 10: 297–302, 2000.
33. **Tonon R and D'Andrea P.** The functional expression of connexin 43 in articular chondrocytes is increased by interleukin 1β: evidence for a Ca^{2+}-dependent mechanism. *Biorheology* 39: 153–160, 2002.
34. **Urbach V, Leguen I, O'Kelly I, and Harvey BJ.** Mechanosensitive calcium entry and mobilization in renal A6 cells. *J Membr Biol* 168: 29–37, 1999.
35. **Vergara L, Bao X, Cooper M, Bello-Reuss E, and Reuss L.** Gap-junctional hemichannels are activated by ATP depletion in human renal proximal tubule cells. *J Membr Biol* 196: 173–184, 2003.
36. **White TW, Bruzzone R, and Paul DL.** The connexion family of intercellular channel forming proteins. *Kidney Int* 48: 1148–1157, 1995.
37. **Yao J, Morooka T, Li B, and Oite T.** Co-ordination of mesangial cell contraction by gap junction-mediated intercellular Ca^{2+} wave. *J Am Soc Nephrol* 13: 2018–2026, 2002.
38. **Yaoita E, Yao J, Yoshida Y, Morioka T, Nameta M, Takata T, Kamiie J, Fujinaka H, Oite T, and Yamamoto T.** Up-regulation of connexin 43 in glomerular podocytes in response to injury. *Am J Pathol* 161: 1597–1606, 2002.